Spectral studies of flaring quasar PKS 1424-418 above 100 MeV with *Fermi*-LAT

Feraol F. Dirirsa[1,*], Richard J. Britto[1] and Soebur Razzaque[1]
on behalf of the *Fermi*-LAT Collaboration

[1] *Department of Physics, University of Johannesburg, P. O. Box 524, Auckland Park 2006, South Africa*

E-mail: *fdirirsa@uj.ac.za

Abstract. The Flat Spectrum Radio Quasar (FSRQ) PKS 1424-418 is an Active Galactic Nucleus (AGN) located at a redshift z = 1.522. This source has shown several flaring episodes through the whole electromagnetic spectrum in recent years. The *Fermi*-Large Area Telescope (*Fermi*-LAT), a space-based gamma-ray detector, has detected four outbursts during the 2012 October to 2013 September period, which were also followed up by the Hartebeesthoek Radio Astronomy Observatory (HartRAO). We present an analysis of *Fermi*-LAT data on PKS 1424-418 during this period. Studies of the flaring pattern of FSRQs, such as PKS 1424-418, can provide interesting constraints related to the physics of the gamma-ray production in these objects.

1. Introduction

The *Fermi* Gamma-Ray Space Telescope has been collecting data from the whole sky since 2008 [1]. The majority of the extragalactic objects observed by *Fermi*'s main instrument—the Large Area Telescope (LAT), are classified as blazars [2]. They constitute a large group of active galaxies that host an active galactic nucleus (AGN). In the popular unification scenario of AGNs, blazars are understood as sources in which a relativistic jet is produced by the central engine and aligned with the observer's line of sight [3]. These objects are marked by a high flux from the radio to the gamma-ray band and their spectral energy distributions (SEDs) are characterized by a double-peak structure [4], one peaking between the Infrared and the X-ray region, the other one at gamma-ray energies. The low energy peak can be widely interpreted as synchrotron radiation from relativistic electrons in the jets, while the second high frequency bump is presumably due to inverse Compton scattering between the same electron population interacting either with the synchrotron soft photons (synchrotron self-Compton process) or with other photons (external Compton process) that originated in the local environment [4].

Currently LAT onboard *Fermi* permits an unprecedented view of the SED and variability of blazars, especially the most powerful flat spectrum radio quasars (FSRQs). In this work, we study spectra of four prominent outburst episodes of the FSRQ PKS 1424-418 ($z = 1.522$) that were detected by *Fermi*-LAT from 2012 October to 2013 September [5]. The Automatic Telescope for Optical Monitoring (ATOM) also provided a dense optical light curve coverage for this source [6]. PKS 1424-418 is a bright, compact radio source and a highly polarized optical quasar. The bulk emission of this radiation may occur in the innermost regions of the AGN,

within the broad-line region (BLR). This source was in an active phase in 2012–2013, during which the large flux allowed us to track the spectral behaviour of the source. Therefore, we study this flaring pattern in order to investigate possible constraints related to the physics of the gamma-ray production in FSRQs.

2. Method and Data processing

We analysed the *Fermi*-LAT data between 2012 October 01 and 2013 September 30, corresponding to the Modified Julian Days (MJD) 56201.0 to 56565.0, using the likelihood analysis package of the standard *Fermi Science Tools* v9r33p0, publicly available at the *Fermi* mission website[1]. We used the *Pass 7 reprocessed* data representation, the "source" event class with energy between 100 MeV and 300 GeV, and the P7REP_SOURCE_V15 instrument response functions. The maximum zenith angle was set to 100° to avoid contamination from the Earth limb. Photons were selected in a circular region of interest (ROI) of 10° radius, centered at the position of the source of interest. We took into account the diffuse backgrounds (modeled using "gll_iem_v05_rev1.fit" for the Galactic diffuse emission and "iso_source_v05.txt" for the isotropic background model).

The Enrico software, an user contributed package built upon the python backbone of the science tools, is also used to analyse the spectral energy distribution of the source of interest. We have performed an unbinned likelihood analysis (using the "gtlike" *Science Tool* [7]) of the *Fermi*-LAT data by using a source model in which the spectrum of all the sources of the third *Fermi*-LAT source Catalog (3FGL) located within a 20° radius from PKS 1424-418 are modeled. The likelihood analysis consist in optimising the value of the spectral parameters of the modeled sources by a maximum likelihood statistics procedure.

In the following sections where our results are presented, the "PRELIMINARY" label was added to the figures, since our results constitute a work in progress that requires further validation within the *Fermi*-LAT Collaboration.

2.1. Spectral energy distribution analysis

SEDs of blazars are well modeled by a log-parabola function. This model has been already used with success to fit the spectra of blazars in the catalog of 157 X-ray SEDs observed with BeppoSAX [8]. The log-parabolic model of equation (1) is one of the simplest ways to represent curved spectra when they do not show a sharp high energy cut-off like that of an exponential. We write the log parabola function as

$$dN(E)/dE = N_0' \left(\frac{E}{E_b}\right)^{-\left(\alpha+\beta\log\left(\frac{E}{E_b}\right)\right)} \text{ ph/(cm}^2 \text{ s keV)}, \quad (1)$$

where N_0' is a prefactor, the α index denotes the slope at $E = E_b$ and the β index models the curvature of the log-parabola[2]. We fixed the reference energy E_b at 415.8×10^3 keV as in 3FGL and therefore the spectrum is completely determined only by the three parameters N_0', α and β. The energy flux is given by

$$F(E) = EdN(E)/dE = EN_0' \left(\frac{E}{E_b}\right)^{-\left(\alpha+\beta\log\left(\frac{E}{E_b}\right)\right)}. \quad (2)$$

[1] http://fermi.gsfc.nasa.gov/ssc/data/analysis/software/

[2] When used as a unit, we abbreviate "photon" as "ph"

Thus to see the energy at which the source luminosity peaks on a logarithmic frequency scale, we have to plot $\log EF(E)(= \nu F(\nu))$ versus $\log E$, *i.e.* the energy flux is then simply written as

$$E^2 dN(E)/dE = (1.60 \times 10^{-9}) E^2 N_0' \left(\frac{E}{E_b}\right)^{-\left(\alpha+\beta \log\left(\frac{E}{E_b}\right)\right)} \text{ erg/(cm}^2 \text{ s)}, \quad (3)$$

where the numerical constant is the energy conversion factor from keV to erg and N_0' is a prefactor, such as $N_0' = N_0/(1.60 \times 10^{-9})$ and N_0 being the prefactor of the spectrum in this rescaled model. A power law with an exponential cut-off (PLExpCutoff) model has also been used in our unbinned likelihood analysis, given by

$$E^2 dN(E)/dE = (1.60 \times 10^{-9}) E^2 N_0' \left(\frac{E}{E_0}\right)^{\gamma_1} \exp\left(-\left(\frac{E}{E_c}\right)\right) \text{erg/(cm}^2 \text{ s)}, \quad (4)$$

where E_0 is the pivot energy at which the error in the differential photon flux is minimal, E_c is the cut-off energy, and γ_1 is the photon spectral index. E_0 was arbitrary fixed at 100 MeV.

2.2. Light curve

Variations in flux of PKS 1424-418 are represented by light curves that we draw in a one-day time binning. Though the spectral shape of this source exhibits a definite curvature, we chose to model it with a simple power law, in order to minimize statistical errors on the photon indices. Since the differential flux of a power law model can be represented by $dN(E)/dE = N_0 (E/E_0)^{-\gamma}$, the integral flux was then computed between 100 MeV and 300 GeV, such as:

$$F(\text{E} > 100 \text{ MeV}) = \int_{100 \text{ MeV}}^{300 \text{ GeV}} N_0 \left(\frac{E}{E_0}\right)^{-\gamma} dE. \quad (5)$$

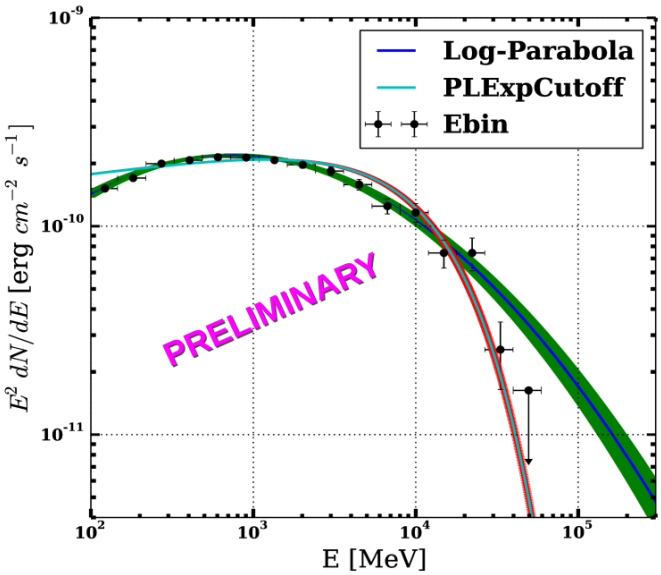

Figure 1. SED of PKS 1424-418, from 2012 October 01 to 2013 September 30 (MJD 56201–56565) fitted with a LP function (fitting parameters: $N_0 = 7.63 \times 10^{-10^{+8.6\times10^{-12}}_{-8.7\times10^{-12}}}$ erg^{-1}cm^{-2} s^{-1}, $\alpha = 1.87 \pm 0.01$, $\beta = 0.11 \pm 0.01$, $E_b = 415.8$ MeV) and a PLExpCutoff function (with fitting parameters: $N_0 = 1.12 \times 10^{-8}$ erg^{-1}cm^{-2} s^{-1}, $E_0 = 100$ MeV, $E_c = 11688^{+865}_{-1146}$ MeV, $\gamma_1 = -2.0$.) The likelihoods of the fitting procedures are given by the values $-loglike = 150379.3$ and 150394.0 for the LP and PLExpCutoff fits respectively.

Table 1. Flaring activity of PKS 1424-418 from 2012 October until 2013 September.

Source periods	Start & Stop date(MJD)	Start & Stop date (UTC)	Duration (days)
Period A	56201.0 – 56257.0	2012 Oct. 01 – 2012 Nov. 26	57
Period B	56257.0 – 56362.0	2012 Nov. 26 – 2013 Mar. 11	105
Period C	56362.0 – 56461.0	2013 Mar. 11 – 2013 Jun. 18	99
Period D_1	56461.0 – 56504.0	2013 Jun. 18 – 2013 Jul. 31	43
Period D_2	56504.0 – 56565.0	2013 Jul. 31 – 2013 Sep. 30	61

Hard spectra have $\gamma < 2$ with peak at high energies, soft spectra have $\gamma > 2$ with peak at low energies and flat spectra with $\gamma = 2$ means the spectrum has a similar amount of power in all spectral bands. In this analysis, the power law model has been used to analyze the light curves that were produced using the gtlike tool.

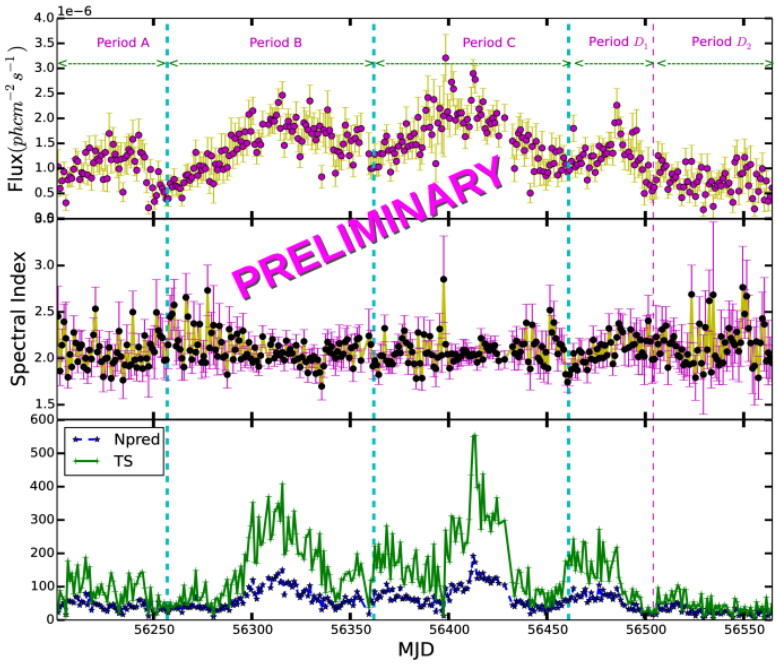

Figure 2. Top panel: Light curve of daily flux (periods categorized according to Table 1). Middle panel: Photon spectral index as a function of time. Bottom panel: TS and N_{pred} versus time.

3. Data analysis

Fig. 1 shows the 12-month averaged SED of PKS 1424-418 (corresponding to the whole data set shown in Table 1), along with the log-parabola and PLExpCutoff functions whose parameters were obtained by the unbinned likelihood analysis.

In Fig. 2, the top panel displays the light curve of the four flaring states of PKS 1424-418 (labeled as A, B, C, D_1) and post-flare (labeled as D_2), over a one-year period of one-day time binning. It exhibits flux variability across a wide time range. A detailed study of these flux variations can provide information on the physics and dynamics of the emitting region. In this

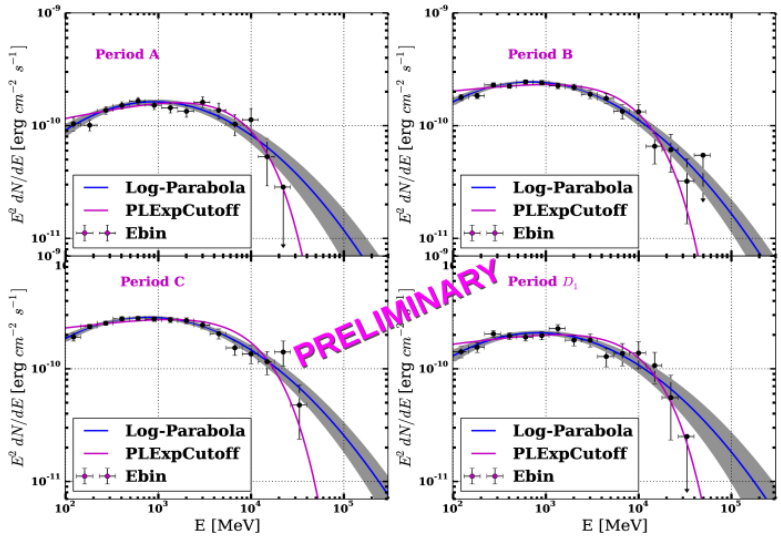

Figure 3. SEDs of four flaring period fitted by LP and PLExpCutoff models from energy range 100 MeV to 300 GeV. Fitting parameters of both models are given in Tables 2 and 3.

Table 2. Unbinned likelihood spectral fitting parameters and derived qualities of fit ($-loglike$) for PKS 1424-418, using the LogParabola (LP) model.

Time Range	N_0 ($\mathrm{erg^{-1}cm^{-2}\ s^{-1}}$)	α	β	E_b (MeV)	$-$loglike	χ^2(ndf)	$\chi^2_{\rm red}$
Period A	$(5.47\times10^{-10})^{+1.85\times10^{-11}}_{-1.81\times10^{-11}}$	1.81±0.04	0.12 ±0.02	415.8	46443.3	12.01(14)	1.33
Period B	$(8.58\times10^{-10})^{+1.67\times10^{-11}}_{-1.64\times10^{-11}}$	1.89±0.02	0.11±0.02	415.8	72051.0	10.45(15)	1.05
Period C	$(9.93\times10^{-10})^{+1.84\times10^{-11}}_{-1.83\times10^{-11}}$	1.87±0.02	0.10±0.01	415.8	67736.0	7.36(15)	0.74
Period D_1	$(5.55\times10^{-10})^{+1.48\times10^{-11}}_{-1.45\times10^{-11}}$	1.85±0.03	0.12±0.02	415.8	38742.6	9.61(15)	0.96

Table 3. Unbinned likelihood spectral fitting parameters and derived qualities of fit ($-loglike$) for PKS 1424-418, using the PLExpCutoff model.

Time Range	N_0 ($\mathrm{erg^{-1}cm^{-2}\ s^{-1}}$)	E_0 (MeV)	E_c (MeV)	γ_1	$-$loglike	χ^2(ndf)	$\chi^2_{\rm red}$
Period A	$(7.30\times10^{-09})^{+5.07\times10^{-10}}_{-5.00\times10^{-10}}$	100.00	9298^{+2291}_{-1716}	$-1.83^{+0.04}_{0.00}$	46442.5	14.65 (14)	1.63
Period B	$(1.28\times10^{-08})^{+4.72\times10^{-10}}_{-4.63\times10^{-10}}$	100.00	11087^{-1938}_{-1534}	−1.91 ±0.02	72058.9	25.20 (15)	2.52
Period C	$(1.45\times10^{-08})^{+5.18\times10^{-10}}_{-5.30\times10^{-10}}$	100.00	12694^{+1990}_{-1711}	−1.90 ±0.02	67742.6	27.83(15)	2.78
Period D_1	$(8.04\times10^{-09})^{+4.37\times10^{-10}}_{-4.30\times10^{-10}}$	100.00	10821^{+2302}_{-1765}	−1.89 ±0.03	38744.2	14.77(15)	1.48

figure, the vertical dashed lines shows the range of the five periods that we identified for an analysis based upon a high flux observed, and the test statistic sketched at the bottom panel in the figure is given by $TS = -2\log L_{\rm max,0}/L_{\rm max,1}$, where $L_{\rm max,0}$ and $L_{\rm max,1}$ are the maximum likelihoods of the model that includes or not the source of interest, respectively, and N_{pred} is the number of photon counts predicted by the optimised model.

As shown in Fig 2, a first flare was observed from the beginning of 2012 October and lasted for almost two months (period A). The second flare was observed in 2013 January, in the middle of period B. It was significantly brighter than the flare detected in 2012 October. The third

flare was observed in 2013 April (middle of period C) with a very high daily flux. The TS and N_{pred} were higher than the values of the previous recorded ones as shown in the bottom panel of Fig. 2. The fourth flaring episode (period D_1) was observed in 2013 July with a high daily flux—around 1×10^{-6} ph cm^{-2} s^{-1}, almost every day of this month. During the post-flare observations (period D_2), the source was fainter, with a photon index ranging between about 1.8 and 2.8. Flaring episodes often spanned from weeks to months, though rapid and intense sub-flares are observed in between.

Fig. 3 shows the SED distributions of PKS 1424-418, along with both the log-parabola (blue line) and PLExpCutoff (marble line) functions whose parameters where obtained by the unbinned likelihood analysis. The parameters of the different fits can be found in the Tables 2 and 3, respectively. The SED shapes have not changed significantly, though flux varied from one flaring episode to another. A particular hint of flattening of the SED was observed when the source became brighter (as shown in Fig. 2, period C). However, the SED is well fitted by a log-parabola function with $\chi^2_{\rm red} = 0.73$ over the whole energy range covered (E > 100 MeV).

Error bars represent the statistical errors while the vertical arrows show upper limits. Upper limits on the flux were calculated when the Test Statistic (TS) value for the source was lower than 9 (significance lower than $\sim 3\sigma$) or when N_{pred} was lower than 3. Results from the photon spectral index study suggest that hardening did not happen when the source was brighter (as it would be if following the general trend of bright FSRQs). There is rather a hint of hardening after the flaring peak of period B. However, statistical uncertainties are too large to clearly exhibit this feature.

4. Summary

The analysis of four flaring periods of PKS 1424-418 during its 2012 October–2013 September outburst was presented. The spectral shapes of this source during the whole period of flaring activities and the post-flaring episode were analysed using two spectral models, namely LP and PLExpCutoff. The spectral analysis were performed using the unbinned maximum likelihood estimator (gtlike science tool). The SEDs of individual flares were plotted and show that the spectrum was also curved during the single flaring episodes. The spectral shapes do not vary significantly between the four flaring episodes despite dramatic flux variations. On the light curve, we do not see higher flux coinciding with the hardening of the photon spectral index.

Acknowledgments

The *Fermi*-LAT Collaboration acknowledges support for LAT development, operation and data analysis from NASA and DOE (United States), CEA/Irfuand IN2P3/CNRS (France), ASI and INFN (Italy), MEXT, KEK, and JAXA (Japan), and the K.A. Wallenberg Foundation, the Swedish Research Counciland the National Space Board (Sweden). Science analysis support in the operations phase from INAF (Italy) and CNES (France) is also gratefully acknowledged. The work presented in this paper was supported in part by an MWGR 2015 grant from the National Research Foundation with Grant No. 93273.

References

[1] Atwood W. B., et al., 2009, *ApJ*, **697**, 1071
[2] Abdo A. A., et al., 2010, *ApJS*, **188**, 405
[3] Dermer C. D., 2014, *Astro-Ph.HE*, **1**, 1408
[4] Massaro E., et al., 2006, *A&A*, **448**, 861-71
[5] Stefano C., et al., 2013, *The Astronomer's Telegram*, **4770**, 1
[6] Buson S., et al., 2014, *A&A*, **40**, A569
[7] http://fermi.gsfc.nasa.gov/ssc/data/analysis/documentation/Cicerone/
[8] Massaro E., et al., 2004, *A&A*, **413**, 489-503.
[9] D'Ammando F., et al., 2013, *The Astronomer's Telegram*, **4714**, 1